OPEN ACCESS Freely available online

PLOS ONE

Emergence of Blind Areas in Information Spreading

Zi-Ke Zhang[1,2]☯, Chu-Xu Zhang[1,3]☯, Xiao-Pu Han[1,2], Chuang Liu[1,2]*

1 Institute of Information Economy, Hangzhou Normal University, Hangzhou, People's Republic of China, **2** Alibaba Research Center for Complexity Sciences, Hangzhou Normal University, Hangzhou, People's Republic of China, **3** Web Sciences Center, University of Electronic Science and Technology of China, Chengdu, People's Republic of China

Abstract

Recently, contagion-based (disease, information, etc.) spreading on social networks has been extensively studied. In this paper, other than traditional full interaction, we propose a partial interaction based spreading model, considering that the informed individuals would transmit information to only a certain fraction of their neighbors due to the transmission ability in real-world social networks. Simulation results on three representative networks (BA, ER, WS) indicate that the spreading efficiency is highly correlated with the network heterogeneity. In addition, a special phenomenon, namely *Information Blind Areas* where the network is separated by several information-unreachable clusters, will emerge from the spreading process. Furthermore, we also find that the size distribution of such information blind areas obeys power-law-like distribution, which has very similar exponent with that of site percolation. Detailed analyses show that the critical value is decreasing along with the network heterogeneity for the spreading process, which is complete the contrary to that of random selection. Moreover, the critical value in the latter process is also larger than that of the former for the same network. Those findings might shed some lights in in-depth understanding the effect of network properties on information spreading.

Citation: Zhang Z-K, Zhang C-X, Han X-P, Liu C (2014) Emergence of Blind Areas in Information Spreading. PLoS ONE 9(4): e95785. doi:10.1371/journal.pone.0095785

Editor: Jesus Gomez-Gardenes, Universidad de Zarazoga, Spain

Received January 3, 2014; **Accepted** March 31, 2014; **Published** April 24, 2014

Funding: This work was partially supported by the National Natural Science Foundation of China (grant numbers 11105024, 11205040, 1147015, 11301490 and 11305043), the EU FP7 Grant 611272 (project GROWTHCOM), the start-up foundation and Pandeng project of Hangzhou Normal University. The funders had no role in study design, data collection and analysis, decision to publish, or preparation of the manuscript.

Competing Interests: The authors have declared that no competing interests exist.

* E-mail: liuchuang@hznu.edu.cn

☯ These authors contributed equally to this work.

Introduction

With the advent of various online Social Networking Services (SNS), the dissemination of information through Internet, also known as *word-of-mouth* or *peer-to-peer* spreading, has attracted much attention for researchers in recent years [1,2]. Following the rapid development of database technology and computational power, various spreading phenomena on large-scale social networks, such as the news [3], rumors [4,5], innovation [6], behavior [7,8], culture [9], viral marketing [10], cooperative behaviors [11] etc, can now be deeply studied in terms of theoretical models as well as empirical analyses.

Generally, the information spreading dynamics is usually studied under the framework of epidemic spreading [12]. Therefore, in many studies, the process of information diffusion is regarded equally as the disease propagation, which informs agents to transmit information to their neighbors via social connections [13]. Among them, the Susceptible-Infected-Recovered (SIR) model is the most commonly used method to describe the information spreading process, where individuals would lose interest of further contribution due to a variety of less predictable factors, which is very similar to the R state of the SIR model in epidemic spreading. The interplay between the spreading dynamics and network structure is a key insight in the study on network spreading dynamics [14,15]. The network structure affects both the spreading speed and prevalence through features such as the shortest path length, degree distribution, degree correlations, and so on. In addition, the upper bound of informed proportion is proved to be approximate to 80% for the SIR model on random networks when the population size is infinite [16]. Previous works have also revealed that there indeed exists a propagation threshold of information spreading on the small-world network [17,18], and the spreading is much faster and broader than that on regular network for the existence of the long-range edges [19]. Moreno *et al.* [5,20] studied the rumor spreading on scale-free networks, and found that the existence of hub nodes can enhance the spreading speed rather than the influenced scope. Recently, there is a vast class of studies focusing on the spreading dynamics on interconnected networks [21], and there is a mixed phase below the critical infection strength in weakly coupled networks [22]. The study of cooperative behaviour spreading across the interdependent networks [23] indicated that interdependent links are more likely to connect two cooperators than the regular links. Furthermore, some interesting phenomena are discovered based on the information diffusion on real social systems, such as the telephone interactions [24,25], tweets [26,27] and emails [24]. Empirical results indicate that the human active patterns [28,29] and the role of weak ties [30] would strongly affect the information spreading.

However, there are also plenty of researches arguing that the underlying mechanism of information diffusion should be fundamentally different from that of epidemic spreading. L*ü et al.* [31] summarized the significant differences between them, and concluded that the information, by considering the social enhancement, would spread more effectively in regular networks than that in random networks. This would to some extent support the real human experiment reported by Centola [7]. Most

theoretical models assumed that the informed agents would transmit the information to all their neighbors [32,33] or just one randomly chosen neighbor [34] in one single time step. However, since passing messages along would take a perceived transmission cost [35] in real societies, the diffusion targets would be selected among individuals with potential interests [36]. Thus, the information flow would travel through social connections thereby depending on the properties of observed networks [37].

In this paper, we propose a theoretical model with considering the effect of partial interaction, where the number of interacted neighbors is in proportion to the spreader's degree. Simulation results show that the spreading process percolates on all three classical networks (ER, BA and WS networks), which is quite similar with the site percolation in statistical physics [38]. In addition, it is observed that the percolation peaks later on WS network than other two networks, which could be regarded as a good explanation of why information can spread more widely on WS network. Furthermore, it is also astonishing to find that the size distribution of unreachable clusters, namely the *Information Blind Area*, exhibits the power-law property, which is the universal phenomenon in the community distribution [39,40].

Models

In this paper, we consider a synthetic network $G(N,E)$, where N is the number of nodes and E is the number of links, representing the individuals and their interactions, respectively. Analogous with the SIR model, every individual would be and only be at one of the three following states during the process of information spreading,

- *Uninformed* (S). The individual has not yet received the information, and is analogous to the susceptible state of the SIR model;
- *Informed* (I). The individual is aware of the information but has not transmitted it, and is analogous to the infected state in the SIR model;
- *Exhausted* (R). After transmitting the information, the individual will probably lose interest and no longer transmit it [41], thus is analogous to the recovered state of the SIR model.

Subsequently, we are mainly interested in the effect of partial interaction. That is to say, each infected node, so-called *spreader* [42], will only influence a certain fraction of its neighbors. Thus, the model can be described as follows.

- Initially, one arbitrary node is randomly picked as the *Information Seed* (I-state) and the rest remain uninformed (S-state).
- Then, the seed will transmit information to α fraction of its neighbors and then becomes exhausted (R-state), where $\alpha \in [0,1]$;
- For simplicity, we assume that all individuals fully trust their social connections. Consequently, each individual will approve the information once s/he receives it;
- After approval, s/he becomes an informed individual or a spreader (I-state), and will transmit the information to all α fraction of her/his neighbors and becomes exhausted (R-state);
- The above process will repeat until there is no individual transmits the information any more.

In this model, the popular individuals (nodes with large degree) tend to interact with more neighbors when they approve the information. However, since there is transmission cost in the spreading process [35], that is to say, individuals would not be able to interact with all their own neighbours. Therefore, we propose a tunable parameter $\alpha \in [0,1]$, representing the interaction strength. Thus, the number of neighbors will be informed, αk, is proportional to the spreader's degree k, neglecting the neighbors' states. And the probability of each neighbor of being selected is $\frac{1}{k}$ at each round, and the repeating selection is prohibited. Figure 1 shows the proposed spreading rule. By setting $\alpha = 0.6$, the informed node I_1 can only transmit information to three neighbors, two uninformed nodes S_1, S_3 and one exhausted node R_1. Therefore, the present rule implies a different feature of information spreading, *Partial Interaction*, which is usually neglected in the standard SIR model and its variants for information spreading. In addition, the immediate influence in the present model corresponds to the two parameters in traditional SIR model, the infected probability β and the recovered probability μ, are both equal to one in the proposed model.

To better investigate the effect of the present model, we perform analyses on three kinds of network: (i) ER network [43]: a random graph where N nodes connected by E edges which are chosen randomly from all the $N(N-1)/2$ possible edges; (ii) BA network [44]: a growing network where each newly added node connects to m old nodes by preferential attachment mechanism; (iii) WS network [45]: Randomly reshuffle links of a regular network with probability γ and result in the small-world network. As a consequence, we generate corresponding BA, ER and WS networks with the same network size $N = 10000$, $m = 3$, $\gamma = 0.5$ and the average degree $\langle k \rangle = 6$. In addition, to alleviate the effect of randomly selecting the spreading *seed*, all simulation results are obtained by averaging over 1000 independent realizations.

Results and Analysis

Exhausted Rate

Denote $P(R)$ as the fraction of exhausted nodes to the network size, obviously, larger $P(R)$ at the stable state indicates broader information spreading, and vice verse. To determine how the introduced parameter α affects the spreading results, we start our analysis from observing the relationship between $P(R)$ and α. Figure 2 shows that, for all the three networks, $P(R)$ is monotonically increasing with α, suggesting a positive correlation

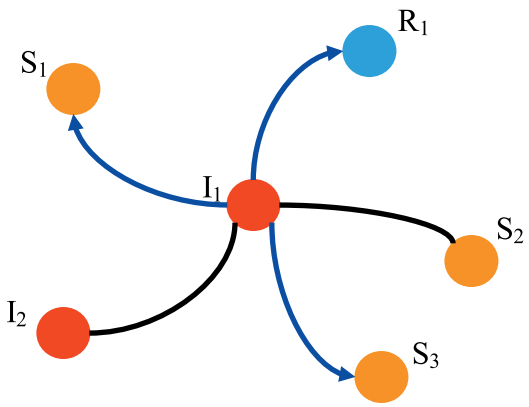

Figure 1. (Color online) **Illustration of the spreading rule in the proposed model with three uninformed nodes, S_1, S_2 and S_3, two informed nodes I_1 and I_2, and one exhausted node R_1.** Each of them has the same probability $\frac{1}{5}$ to receive information from the informed node I_1 at each round. When $\alpha = 0.6$, only $\alpha k = 3$ nodes, e.g. S_1, S_3 and R_1, will receive information.
doi:10.1371/journal.pone.0095785.g001

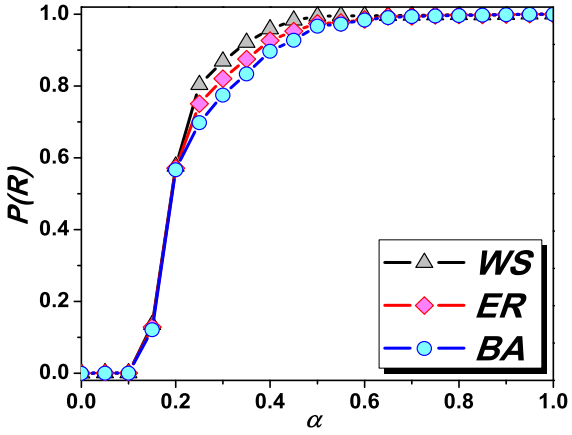

Figure 2. (Color online) **The ratio of exhausted nodes** $P(R)$ **as a function of** α **for three observed networks.**
doi:10.1371/journal.pone.0095785.g002

$P(R)$ and α. As a consequence, in the following, we will use $P(R)$ instead of α to give comprehensive discussions.

Figure 3 reports the model results. In Figure 3a, it shows the dynamics of $P(R)$ on three different networks with the fixed parameter $\alpha=0.35$. It can be seen that WS network yields the most efficient spreading as the largest $P(R)$ at the stable state, while BA network exhibits the narrowest spreading, and ER network stays moderately. This result agrees with previous studies [31]. In addition, the inset shows the dynamic difference of $P(R)$ between two continuous time steps, denoted as $\Delta P(R)=P(R_{t+1})-P(R_t)$, which can be considered as the spreading speed. It indicates that information spreads faster at its initial stage while slows down at later time steps due to the influence of hub nodes. From the degree distribution of Figure 3c, it can be seen that BA network is occupied by more large-degree nodes than other two. Therefore, information spreading on BA network is the fastest while slowest on WS network. According to the partial interaction in the present model, informed agents transmit information to only a certain fraction of their neighbors. Consequently, there would be also some uninformed individuals remaining without receiving any news because they are surrounded by exhausted neighbors (see Figure 4). Considering that the spreading process may influence differently to different type of nodes, we observe the relationship between exhausted rate $P(R_k)$ and node degree k of three networks at the stable state (see Figure 3b), where $P(R_k)$ is the ratio of the total number of exhausted nodes with degree k to the overall number of nodes with degree k. It clearly shows that $P(R_k)$ and k are apparently positively correlated, and nodes with smaller degree have less probability to receive information. Furthermore, Figure 3c displays the degree distributions of three networks. In general, BA network shows the power-law degree distribution where most nodes are of low degree but still a few hub nodes exist due to the *rich-get-richer* mechanism. Poisson degree distribution emerges in ER network because of purely random attachment. Comparatively, most nodes in WS have moderate degree and only a few small and large degree nodes, resulting from the rewiring process. In a word, the generally different fraction of hub nodes (Figure 3c) and different spreading effects on different type of nodes (Figure 3b) support the result of Figure 3a from the perspectives of structure and function, respectively.

Information Blind Areas

As can be seen from Figure 3a, the exhausted rate is always less than 1, suggesting that some nodes will never be informed during the whole spreading process. Specifically, in this paper, we name the region consists of such unreachable nodes as the *Information Blind Area*. Actually, such blind areas emerge regularly due to the spreading process. Figure 4 shows two typical kinds of information blind areas. One is composed by a single uninformed node surrounded by exhausted neighbors and thus it could not receive news. As shown in Figure 4a, the uninformed node S_1 is enveloped by three exhausted nodes R_1, R_2 and R_3, who would neither directly transmit information to S_1 nor allow the informed agents to contact S_1. The other one is composed of multiple uninformed nodes connected with each other and surrounded together by exhausted nodes. Thus, the information will never be transmitted to such a cluster as no path is available. As shown in Figure 4b, three uninformed nodes, S_1, S_2 and S_3, compose a connected cluster which is surrounded by five exhausted nodes, R_1, R_2, R_3, R_4 and R_5. Since no single uniformed node in this cluster can access the outside information world, they have to passively keep *blind* for the spreading information.

In order to describe those two kinds of information blind areas more clearly, we conduct experiments with $N=100$ and $\langle k\rangle=6$. Figure 5 shows the visualization results on the three representative networks. It can be seen that most uninformed individuals at stable state (Figure 5a, 5d, 5g) are generally small-degree ones, which is consistent with the foregoing analysis. In addition, we also show the two information blind areas. The single-node case is displayed in Figure 5b, Figure 5e, Figure 5h. In Figure 5b, the uninformed individual #66 is surrounded by exhausted neighbors #7, #10, #36, #71, #75 and #83. As a consequence, node #66 is prevented from hearing news by its neighbors. Figure 5e and Figure 5h are similar to that of Figure 5b. On the other hand, Figure 5c, 5f, and 5i report the information blind areas of multi-nodes cases on BA, ER and WS networks, respectively. As shown in Figure 5c, three uninformed individuals #49, #86 and #97 compose a connected cluster, which is surrounded by exhausted individuals #1, #4, #7, #17, #18, #35, and #61. Therefore, all the nodes in this relatively large area will not be informed and keep blind to spread information. Similar phenomena can also be discovered in Figure 5f and Figure 5i on ER and WS networks, respectively.

Scale-free Effect

In this section, we shall explain how such blind areas emerge from the perspective of site percolation. Generally, in a typical site percolation system, each node in the given network would be at one of two given states: *empty* with probability p or *occupied* with probability $1-p$, and all the edges connecting with empty nodes are cut off. Previous studies have proved that the site percolation system would display a phase transition phenomenon from *connected* phase to *disconnected* phase when p grows to a critical point p_c [46]. At this point, the behavior of the ratio of giant cluster size (the largest connected cluster) r_g ($r_g=N_g/N$, where N_g is the size of the giant cluster) indicates the network's sudden disintegration, and the scaling distribution of connected clusters would emerge [47–51]. Figure 6a–6c respectively show how r_g changes according to different p, as well as the critical point (see insets) in three different networks (BA, ER and SW networks) with the same network size $N=10000$.

Note that, the role of the empty nodes in site percolation is quite similar with that of the R-state individuals in the present model, where the information blind areas are divided by those individuals. For the R-state individuals are all connected in the proposed

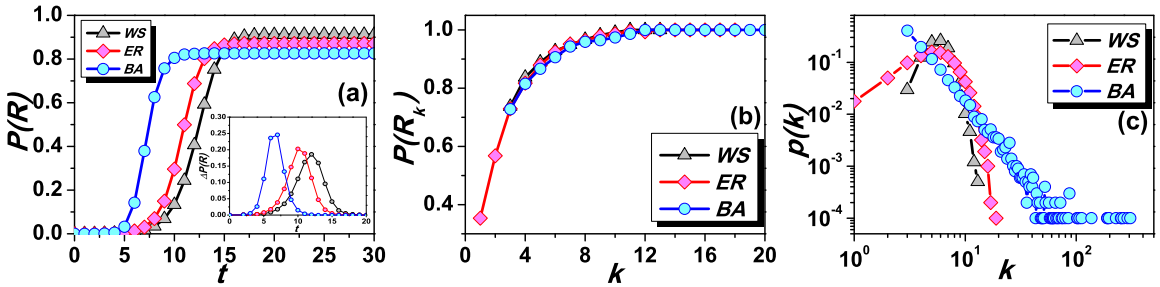

Figure 3. (Color online) **The dynamics of spreading on three networks.** (a) Exhausted rate $P(R)$ as a function of simulation time. Inset is $\Delta P(R)$ as the function of simulation time; (b) Exhausted rate as a function of the node degree; (c) Degree distributions of three networks in log-log scale. The parameter α is set to 0.35 for (a) and (b).
doi:10.1371/journal.pone.0095785.g003

model, we set nodes in the largest connected subgraph in site percolation system as the empty state. Analogous with observing the giant cluster in site percolation, we consequently calculate the ratio of the largest blind area size r_s ($r_s = N_s/N$, where N_s is the size of the largest information blind area) for various exhausted rate $R \in [0,1]$. The results are shown in Figure 6d–6f, where the curve exhibits a very similar trend with that of r_g. In addition, we numerically calculate the thresholds of both p_c and R_c, according to the peak of the relative variance of the size distribution. We denote it by $\chi = \frac{\langle N_c^2 \rangle - \langle N_c \rangle^2}{\langle N_c \rangle}$, where N_c is the size of each connected cluster except the giant one [52], for it would result in large fluctuation when p or R approaches the critical point, and the insets of Figure 6a–6f show the corresponding results. Furthermore, in different networks (BA, ER and WS), we find good agreements between the size distributions of connected clusters and information blind areas of the two respective models. Figure 6g–6i show that the distributions of the connected clusters' size of the two models are coincident with almost the same exponent -2.9 at their respective critical points, indicating that they have very similar critical phenomena.

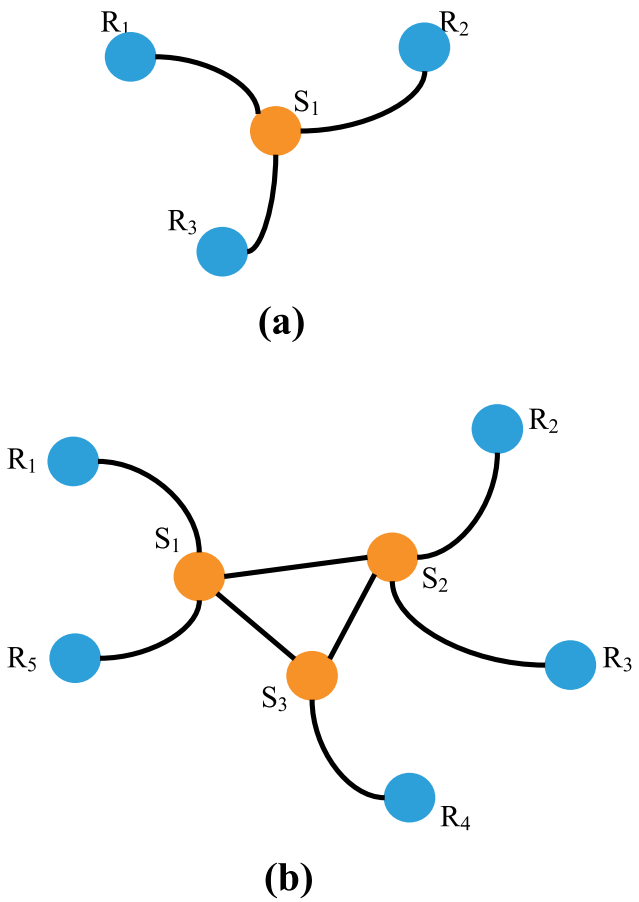

Figure 4. (Color online) **Illustration of two typical kinds of information blind areas: (a) one single-node case; and (b) example of multiple nodes.**
doi:10.1371/journal.pone.0095785.g004

Despite those similar properties, we should not regard the present model as an equivalent process as the site percolation. One significant difference between them is that, the node states are changed according to the diffusion process based on the given network structure in the spreading model, while the site percolation process only randomly label the node states regardless of the network structure. Therefore, the critical points exhibit very differently for the two models. In the insets of Figure 6a–6c, the critical values follow $p_c^{BA} > p_c^{ER} > p_c^{WS}$ for the site percolation, while a completely opposite sequence for the proposed model as shown in the insets of Figure 5d–5f (that is $R_c^{BA} < R_c^{ER} < R_c^{WS}$). For the random labeling process, the more heterogeneous the network is, the larger the critical point will be, as there are more small-degree nodes when each one is treated equally. On the contrary, if there exist some large-degree nodes dominating the network center, messages can be easily spread out via those core nodes, hence the critical point will be smaller for such large heterogeneous network in the diffusion process. Similar statements can also be applied in illustrating that, for the same network, the critical value of the interaction model is always smaller than that of site percolation, e.g. $p_c^{BA} > R_c^{BA}$, $p_c^{ER} > R_c^{ER}$ and $p_c^{WS} > R_c^{WS}$. In a word, although the site percolation principle can not be fully projected to spreading dynamics, it still provides a promising and versatile tool to explain the critical phenomenon of the emergence of blind areas in information spreading.

Conclusions & Discussion

In this paper, we have applied the partial interaction effect in the classical SIR model where three types of node states are considered: (1) Uninformed (S); (2) Informed (I); (3) Exhausted (R). Subsequently, we adopt it in an information spreading scenario, where the interaction strength is proportional to each spreader's degree. Numerical experiments show that there is a clearly positive relationship between the interaction strength and final coverage of

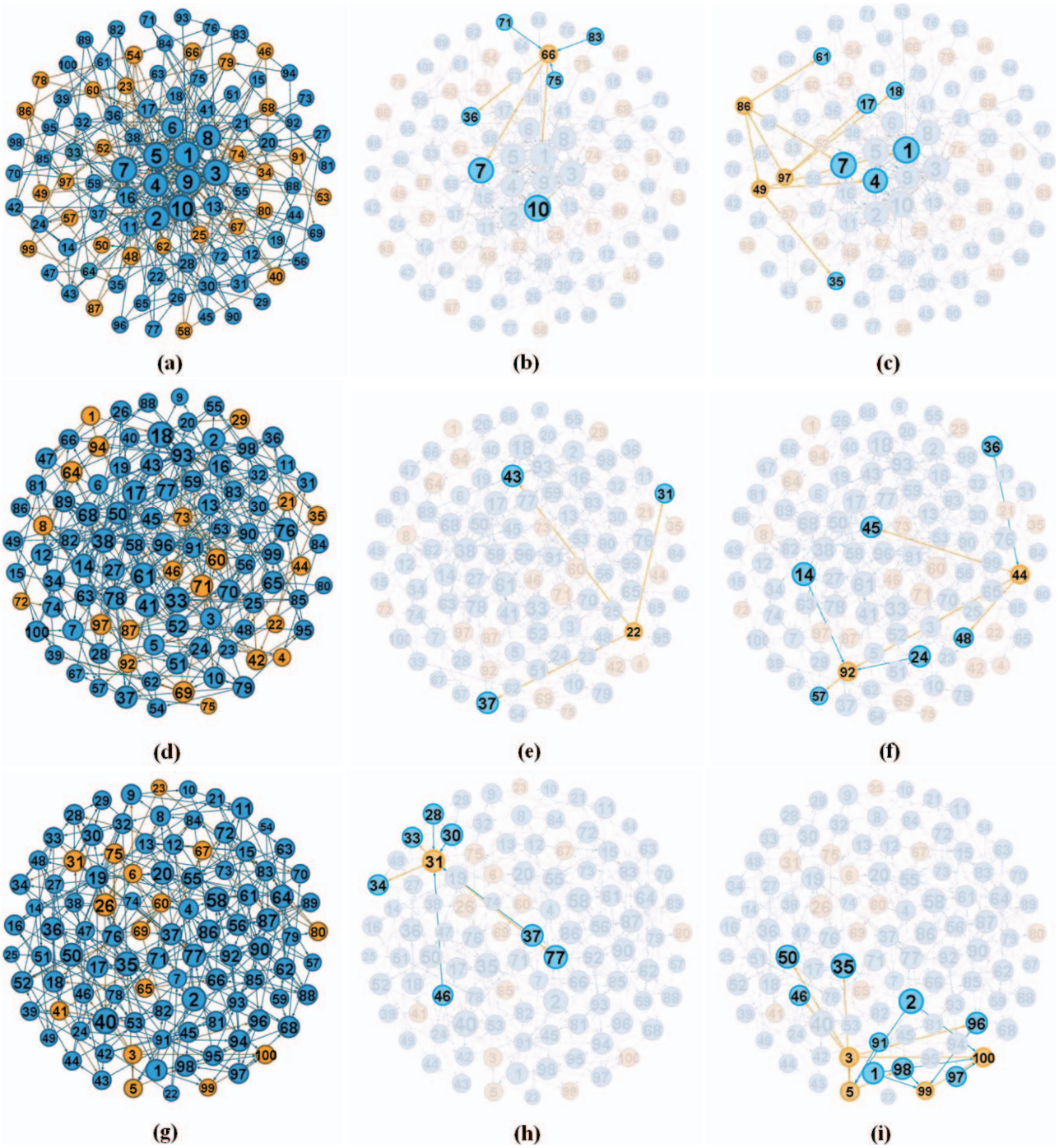

Figure 5. (Color online) **Visualization of information blind areas resulted from designed experiments.** Yellow and blue circles represent the uninformed and exhausted nodes, respectively. The size of each node is proportional to its degree. In addition, (a–c) are the results on BA network; (d–f) are the results on ER network; (g–i) are the results on WS network.
doi:10.1371/journal.pone.0095785.g005

spreading. In addition, we find that the spreading effect is highly influenced by the network structure. One interesting property will result from the spreading process, where the network is divided into several information-unreachable areas, namely *Information Blind Areas*. Analysis reveals that a phase transition of such blind areas' size distribution will emerge when the fraction of R-state individuals grows to a certain critical point. In spite of quite similar results from site percolation analysis, detailed experiments show that the diffusion process is significantly different from random selection. Further numerical analyses on three representative networks (BA, ER and WS) demonstrate that, for the spreading process, the more heterogeneous the network is, the smaller the critical point will be. By contrast, the random labeling process of site percolation is completely opposite. Moreover, the critical value of network-based diffusion is smaller than that of purely random selection. Those findings can be regarded as additional explana-

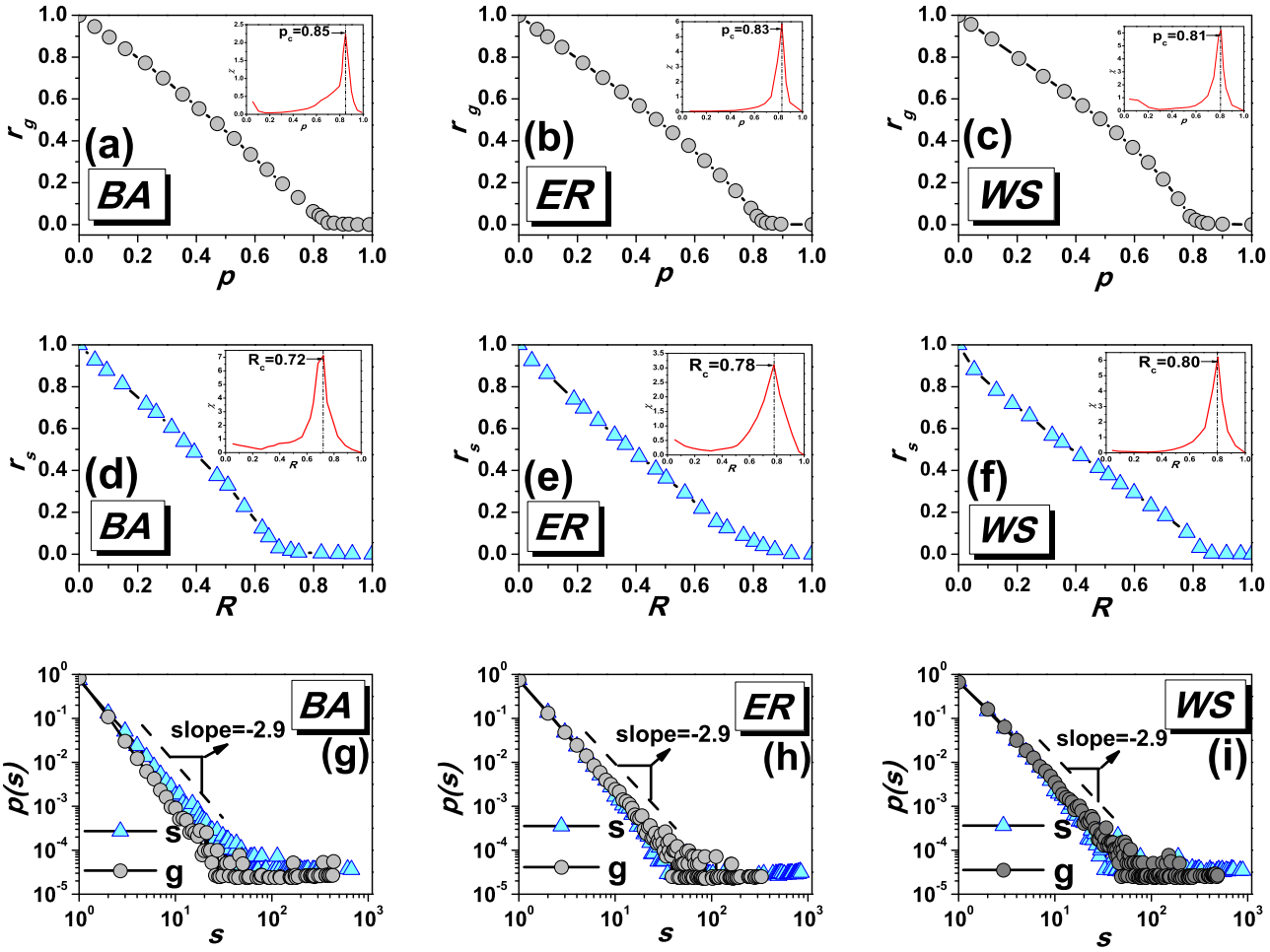

Figure 6. (Color online) **Comparisons between the present model and the site percolation system.** (a–c) The relationship between the size of giant cluster and empty probability p. Inset shows χ versus p, and the peak is the critical point p_c; (d–f) The relationship between the size of the largest information blind areas and the exhausted rate R. Inset shows χ versus R, and the peak is the critical point R_c; (g–i) The size distributions of connected clusters of the two models.
doi:10.1371/journal.pone.0095785.g006

tion why small-world network yields the most efficient information/epdemic spreading in previous studies [19,31].

Recently, the research of both contagion-based spreading models and applications has attracted more and more attention [24,37]. Numerical results in this paper demonstrate that, due to the various network structure, there are always unreachable individuals. Human communication pattern analysis [25,53] would be a promising method to help in understanding how to lighten the *Dark Corners*. In addition, activation of *Long-tail* individuals and products would also enhance the efficiency of *Information Filtering* [54] in the era of big data to solve the *cold-start* dilemma [55,56].

Author Contributions

Conceived and designed the experiments: ZKZ CXZ XPH CL. Performed the experiments: ZKZ CXZ. Analyzed the data: ZKZ CXZ XPH CL. Contributed reagents/materials/analysis tools: CXZ CL. Wrote the paper: ZKZ CXZ XPH CL.

References

1. Van Mieghem P, Van de Bovenkamp R (2013) Non-markovian infection spread dramatically alters the susceptible-infected-susceptible epidemic threshold in networks. Phys Rev Lett 110: 108701.
2. Holme P, Saramäki J (2012) Temporal networks. Phys Rep 519: 97–125.
3. Chen YY, Chen F, Gunnell D, Yip PSF (2013) The impact of media reporting on the emergence of charcoal burning suicide in taiwan. PLoS ONE 8: e55000.
4. Doer B, Fouz M, Friedrich T (2012) Why rumors spread so quickly in social networks. Commun ACM 55: 70–75.
5. Moreno Y, Nekovee M, Pacheco AF (2004) Dynamics of rumor spreading in complex networks. Phys Rev E 69: 066130.
6. Montanari A, Saberi A (2010) The spread of innovations in social networks. Proc Natl Acad Sci USA 107: 5334–5338.
7. Centola D (2010) The spread of behavior in an online social network experiment. Science 329: 1194–1197.
8. Centola D (2011) An exerimental study of homophily in the adoption of health behavior. Science 334: 1269–1272.
9. Dybiec B, Mitarai N, Sneppen K (2012) Information spreading and development of cultural centers. Phys Rev E 85: 056116.
10. Aral S (2011) Identifying social influence: a comment on opinion leadership and social contagion in new product diffusion. Marketing Sci 30: 217–223.
11. Jiang LL, Perc M, Wang WX, Lai YC, Wang BH (2011) Impact of link deletions on public cooperation in scale-free networks. EPL 93: 40001.
12. Daley DJ, Kendall DG (1964) Epidemics and rumors. Nature 204: 1118.
13. Castellano C, Fortunato S, Loreto V (2009) Statistical physics of social dynamics. Rev Mod Phys 81: 591–646.

14. Zhou T, Fu ZQ, Wang BH (2006) Epidemic dynamics on complex networks. Prog Nat Sci 16: 452–457.
15. Nagata K, Shirayama S (2012) Method of analyzing the influence of network structure on information diffusion. Physica A 391: 3783–3791.
16. Sudbury AJ (1985) The proportion of the population never hearing a rumour. J Appl Prob 22: 443–446.
17. Zanette DH, Argentina RN (2001) Critical behavior of propagation on small-world networks. Phys Rev E 64: 050901.
18. Stone TE, Mckay SR (2011) Critical behavior of disease spread on dynamic small-world networks. EPL 95: 38003.
19. Keeling MJ, Eames KTD (2005) Networks and epidemic models. J R Soc Interface 2: 295–307.
20. Moreno Y, Nekovee M, Vespignani A (2004) Efficiency and reliability of epidemic data dissemination in complex network. Phys Rev E 69: 055101.
21. Gao JX, Buldyrev SV, Stanley HE, Havlin S (2012) Networks formed from interdependent networks. Nat Phys 8: 40–48.
22. Dickison M, Havlin S, Stanley HE (2012) Epidemics on interconnected netwoks. Phys Rev E 85: 066109.
23. Jiang LL, Perc M (2013) Spreading of cooperative behaviour across interdependent groups. Sci Rep 3: 2483.
24. Karsai M, Kivelä M, Pan RK, Kaski K, Kertész J, et al. (2011) Small but slow world: How network topology and burstiness slow down spreading. Phys Rev E 84: 046116(R).
25. Miritello G, Moro E, Lara R (2011) Dynamical strength of social ties in information spreading. Phys Rev E 83: 045102(R).
26. Goel S, Watts DJ, Goldstein DJ (2012) The structure of online diffusion network. In: Proc. 13th Int. Conf. EC. NewYork: ACM, pp. 623–638.
27. Myers S, Zhu CG, Leskovec J (2012) Information diffusion and external influence in networks. In: Proc. 18th Int. conf. KDD. New York: ACM, pp. 33–41.
28. Iribarren JL, Moro E (2012) Impact of human activity patterns on the dynamics of information diffusion. Phys Rev Lett 103: 038702.
29. Doerr C, Blenn N, Van Mieghem P (2013) Lognormal infection times of online information spread. PLoS ONE 110: e64349.
30. Zhao JC, Wu JJ, Xu K (2010) Weak ties: subtle role of information diffusion in online social networks. Phys Rev E 80: 016105.
31. Lü L, Chen DB, Zhou T (2011) The small world yields the most effective information spreading. New J Phys 13: 123005.
32. Pastor-Satorras R, Vespignani A (2001) Epidemic spreading in scale-free networks. Phys Rev Lett 86: 3200.
33. Sun Y, Liu C, Zhang CX, Zhang ZK (2014) Epidemic spreading on weighted complex networks. Phys Lett A 378: 635–640.
34. Yang Z, Zhou T (2012) Epidemic spreading in weighted networks: An edge-based mean-filed solution. Phys Rev E 85: 056106.
35. Banerjee AV (1993) The economics of rumours. Rev Econ Stud 60: 309–327.
36. Wu F, Hurberman BA, Adamic LA, Tyler FR (2004) Information flow in social groups. Physica A 337: 327–335.
37. Iribarren JL, Moro E (2011) Branching dynamic of viral information spreading. Phys Rev E 84: 046116.
38. Parshani R, Carmi S, Havlin S (2010) Epidemic threshold for the Susceptible-Infectious-Susceptible model on random networks. Phys Rev Lett 104: 258701.
39. Clauset A, Newman MEJ, Moore C (2004) Finding community structure in very large networks. Phys Rev E 70: 066111.
40. Radicchi F, Castellano C, Cecconi F, Loreto V, Parisi D (2004) Defining and identifying communities in networks. Proc Natl Acad Sci USA 101: 2658–2663.
41. Liu C, Zhang ZK (2014) Information spreading on dynamic social networks. Commun Nonliear Sci Numer Simulat 19: 896–904.
42. Kitsak M, Gallos L, Havlin S, Liljeros F, Muchnik L, et al. (2010) Identification of influential spreaders in complex networks. Nat Phys 11: 888–893.
43. Erdös P, Rényi A (1959) On random graphs. Publ Math 6: 290–297.
44. Barabási AL, Albert R (1999) Emergence of scaling in random networks. Science 286: 509–512.
45. Watts DJ, Strogatz SH (1998) Collective dynamics in 'small-world' networks. Nature 393: 440–442.
46. Dorogovtsev SN, Goltsev AV, Mendes JF (2008) Critical phenomena in complex networks. Rev Mod Phys 80: 1275.
47. Newman ME, Watts DJ (1999) Scaling and percolation in the small-world network model. Phys Rev E 60: 7332.
48. Cohen R, Erez K, Ben-Avraham D, Havlin S (2000) Resilience of the internet to random breakdowns. Phys Rev Lett 85: 4626.
49. Albert R, Jeong H, Barabási AL (2000) Error and attack tolerance of complex networks. Nature 406: 378–382.
50. Cohen R, Ben-Avraham D, Havlin S (2002) Percolation critical exponents in scale-free networks. Phys Rev E 66: 036113.
51. Schwartz N, Cohen R, Ben-Avraham D, Barabási AL, Havlin S (2002) Percolation in directed scale-free networks. Phys Rev E 66: 015104.
52. Ferreira SC, Castellano C, Pastor-Satorras R (2012) Epidemic thresholds of the susceptibleinfected-susceptible model on networks: A comparison of numerical and theoretical results. Phys Rev E 86: 041125.
53. Jiang ZQ, Xie WJ, Li MX, Podobnik B, Zhou WX, et al. (2013) Calling patterns in human communication dynamics. Proc Natl Acad Sci USA 110: 1600.
54. Lü L, Medo M, Yeung CH, Zhang YC, Zhang ZK, et al. (2012) Recommender systems. Phys Rep 519: 1–49.
55. Qiu T, Chen G, Zhang ZK, Zhou T (2011) An item-oriented recommendation algorithm on coldstart problem. EPL 95: 58003.
56. Qiu T, Zhang ZK, Chen G (2013) Information filtering via a scaling-based function. PLoS ONE 8: e63531.